

*The Evolution of Galaxies on Cosmological Timescales*  
*ASP Conference Series, Vol. 3 × 10<sup>8</sup>, 1999*  
*J. E. Beckman, and T. J. Mahoney, eds.*

## **Extragalactic radio source evolution & unification: clues to the demographics of blazars**

C A Jackson

*Research School of Astronomy & Astrophysics, The Australian National  
University, Cotter Road, Weston Creek, ACT 2611, Australia*

J V Wall

*Department of Astrophysics, University of Oxford, Nuclear and  
Astrophysics Laboratory, Keble Road, Oxford OX1 3RH, UK*

### **Abstract.**

In this paper we discuss the demographics of the radio blazar population: (i) what are their parent ('unbeamed') sources and (ii) what magnitude and/or type of evolution have they undergone? The discussion is based on models of radio source evolution and beaming based on a 'dual population' unification paradigm. These models, developed from radio blazar properties in bright samples, predict blazar demographic trends at the lower flux-density levels; samples from deep mJy-level surveys (*e.g.* NVSS and FIRST) may now provide direct tests of these predictions.

### **1. Dual-population Unification**

All galaxies are radio galaxies in a sense. The scale of activity ranges from 'normal' galaxies (like our own) whose radio emission emanates from supernova remnants. At higher radio powers are the 'starburst' galaxies, greatly-enhanced stellar activity resulting in stronger radio emission. At similar radio powers are the Seyfert galaxies with their small-scale radio core-jet structures and with clear indication of AGN activity. At the top end of the scale are the powerful radio galaxies, together with BL Lacs and quasars, the latter two being collectively termed blazars.

Radio galaxies tend to have steep radio spectra and therefore dominate low radio-frequency ( $\nu < 0.5$  GHz) surveys. The structures are predominantly double-lobed; Fanaroff & Riley (1974) compared the distances between central maxima of the radio structures to overall size and discovered a dichotomy. Sources with regions of maximum brightness separated by more than 0.5 times the overall source size are edge-brightened (FR II), while when the regions of maximum brightness lies within this limit the source has diffuse outer lobes (FR I) (centrally concentrated); and the highest radio power objects are *predominantly* FR IIs whilst those of lower radio power are *usually* FR Is. The overlap between the classes at middling radio powers is seen in the local radio luminosity function (Figure 1), and the division is known to be a function of optical luminosity as well as radio (Owen and Ledlow 1993).

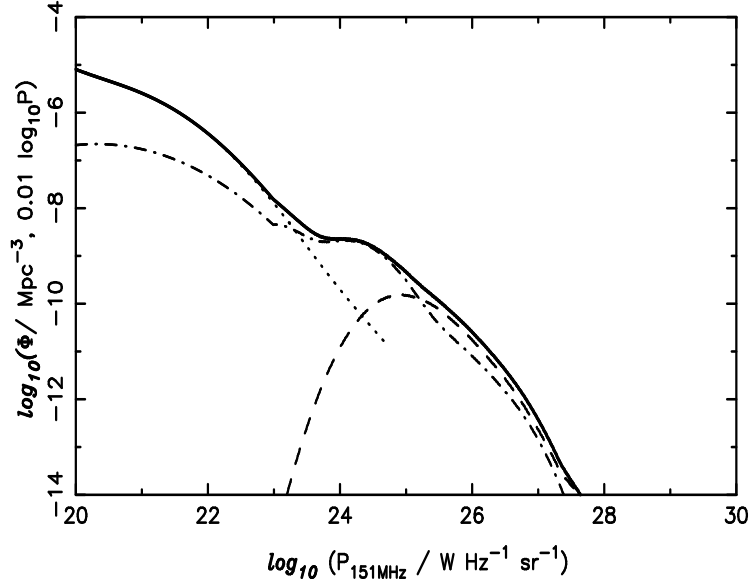


Figure 1. The local radio luminosity function at 151 MHz (dark, solid line) comprises contributions from 3 populations: starburst galaxies (dotted), FRI (dot-dash) and FRII radio galaxies (dashed).

Evidence is accumulating that the powerful radio sources, double-lobed radio galaxies on the one hand and blazars on the other, are ‘unified’ by projection effects, with a central torus together with relativistic beaming responsible for our classification of objects as radio galaxies or blazars (Scheuer & Readhead 1979; Orr & Browne 1982; Scheuer 1987, Barthel 1989, Urry & Padovani 1995 and references therein). The ‘dual-population’ unified scheme (Wall & Jackson 1997), summarised in Table 1, posits that FRII radio galaxies are the parent population of *all* quasars and *some* BL Lac type objects. The FRII-quasar sources are galaxies with class ‘A’ spectra (Hine & Longair, 1979), having strong, high-excitation emission lines in their optical/UV spectra. The FRII-BL Lac sources are galaxies with class ‘B’ spectra (Hine & Longair, 1979), having only weak, if any, high-excitation lines in their spectra. The second part of the scheme posits that FRI radio galaxies are the parent population of the remainder of the BL Lac type objects.

## 2. The cosmic evolution of the parent populations

Our analysis interprets radio source counts and identification/redshift data for samples at high flux densities, adopting a dual-population unified scheme paradigm. Using a simple parametric model to describe the evolution of the underlying parent populations we first fit low-frequency radio data ( $\nu < 0.5$  GHz), where radio samples are unbiased by the effects of Doppler beaming. Then, using these evolution models for the parent populations of FRI and FRII objects, we fit the 5 GHz radio source count using a small number of parameters

Table 1. Unified classes of powerful extragalactic radio sources

Population	UV/optical emission type	Radio spectrum at 5 GHz	Source type
FRII, class A	narrow	steep	RG
	broad	steep	RG
	broad	‘flat’	Quasar
FRII, class B	weak/none	steep	RG
	none	‘flat’	BL Lac
FRI	weak/none	steep	RG
	none	‘flat’	

to describe the Doppler beaming, which gives rise to blazars (*i.e.* quasars and BL Lacs with  $\alpha_{2.7\text{GHz}}^{5\text{GHz}} > -0.5$ , where  $S \propto \nu^\alpha$ )<sup>1</sup>

The fundamental dataset to our analysis is the differential radio source count, the count at a single observing frequency of source density on the sky as a function of flux density. Compiling data from wide-area and deep pencil-beam surveys yields source counts spanning 2 decades in frequency and 6 decades in flux density as shown in Figure 2.

In fact radio source counts contain a wealth of cosmological information, in particular providing potent evidence against a steady-state Universe (Ryle & Clarke 1961) and indicating that differential evolution must take place, with the most luminous sources showing the strongest evolution. In addition the *shape* of the source count changes with observing frequency, suggesting that more complex behaviour than just number density evolution is taking place - and our analysis shows just what this behaviour is.

Identification programmes and further studies of radio source samples have revealed distinct regions within the counts. These regions are indicated along the abscissa in Figure 2 and discussed briefly here:

**Region 1** At the very highest flux densities the source count is near-Euclidean, although typically less than 20 sources contribute to this region. This region is comprised of a mixture of nearby sources and cosmologically-distant powerful sources. The flat count arises due to the dilution of the powerful evolving sources by the local lower-radio-power sources which are far more abundant at low redshifts.

**Region 2** In this region the counts rise more rapidly with decreasing flux density than the Euclidean (-3/2 power law) prediction, and then reach a

<sup>1</sup>Note that our definition of blazar is solely a radio definition and says nothing about the optical equivalent width criteria.

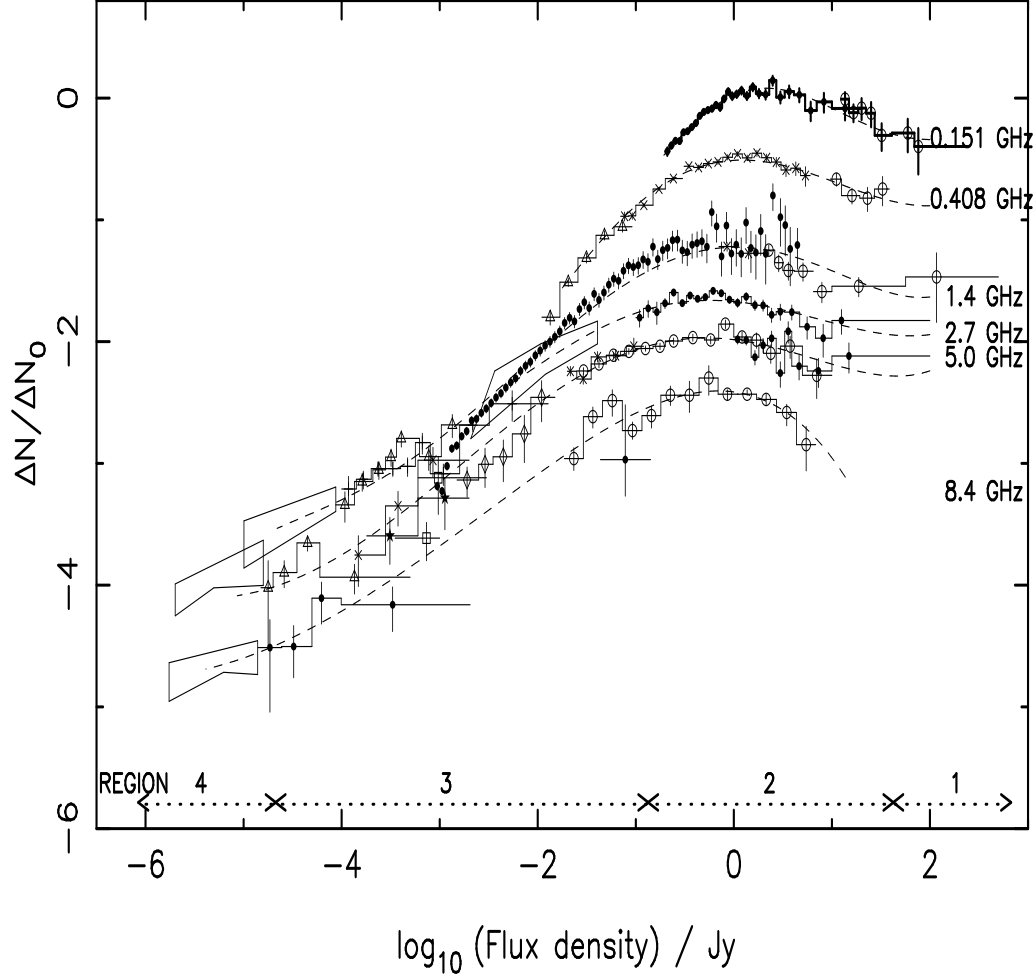


Figure 2. Source counts in relative differential form  $\Delta N / \Delta N_0$  where  $\Delta N$  is the number of sources per sterad with flux density  $S_\nu$  between  $S_2$  and  $S_1$  and  $\Delta N_0$  is the number of sources expected in a uniformly-filled Euclidean universe ( $N_0 = K_\nu S_\nu^{-3/2}$  with  $K_\nu = 2400, 2730, 3618, 4247, 5677$  and  $3738$  for the six frequencies shown). The horizontal bars show the flux-density bin width,  $S_2$  to  $S_1$  and the vertical error is the  $\sqrt{N}$  error. The curves are polynomial least-square fits to the counts. The counts are compiled from radio survey data described in Wall (1994).

Euclidean plateau. This region of the count is made up of the most powerful radio sources at cosmological distances. The low-frequency counts ( $< 0.5$  GHz) comprise almost entirely of steep-spectrum sources whose radio emission is greatest at these frequencies. The width of the plateau increases with increasing frequency, due to an increasing blazar (flat-spectrum) contribution.

**Region 3** Below the Euclidean plateau the counts at all wavelengths drop away from the Euclidean prediction. This region extends up to two orders of magnitude in flux density. (Limited) identification data shows that the sources at such flux densities are lower-power objects at intermediate redshifts and not, as might be supposed, powerful radio sources at ever-increasing redshifts. Very little work has been done on the blazar population at these flux density levels.

**Region 4** At low flux densities the counts again flatten to near-Euclidean. In this region the dominant populations change dramatically to ‘blue’ starburst galaxies and ‘red’ FRI-type galaxies, both relatively local and of low radio powers (*e.g.* Windhorst et al. 1993, Benn et al. 1993).

Using the spectroscopically-complete 3CRR sample at 178 MHz (Laing, Riley & Longair 1983 and more recently published data collated by R. Laing, private communication) we first determine an appropriate form for the evolution of the FRI and FRII populations using the  $\langle V/V_{max} \rangle$  statistic.

Figure 3 shows  $V/V_{max}$  values for 137 steep-spectrum FRII radio galaxies and 26 FRI radio galaxies. Both populations show increasing  $\langle V/V_{max} \rangle$  with radio power. However, FRIs exhibit negative evolution with  $\langle V/V_{max} \rangle < 0.5$  at  $\log_{10}(P_{151 \text{ MHz}} \sim 25.0)$  and the FRIIs exhibit strong positive evolution with  $\langle V/V_{max} \rangle > 0.7$  at  $\log_{10}(P_{151 \text{ MHz}} \sim 27.5)$ . Interestingly, there is a trend for  $\langle V/V_{max} \rangle$  to continuously increase with  $\log_{10}(P_{151 \text{ MHz}})$  across the populations, suggesting luminosity-dependent evolution which may be population-independent.

Adopting exponential luminosity-dependent density evolution (LDDE) we fit the source count at 151 MHz comprising the 3CRR and 6C survey (Hales, Baldwin, & Warner 1988), using a minimisation routine. The model fit requires strong evolution of the most powerful FRII sources, with little or no evolution of the FRI population (Table 2). Thus the fit reproduces the  $\langle V/V_{max} \rangle$  behaviour for the radio galaxy population as a whole, in that only FRIIs with  $\log_{10}(P_{151 \text{ MHz}}) > 25.44$  undergo any evolution, the lower-power FRIIs and all FRIs have a constant space density to their cut-off redshift,  $z_c$ .

### 3. Blazars from beamed parent radio sources

We fit the 5 GHz source count, which is well-defined over a wide flux-density range, starting from the evolution model fit of Table 2. However at 5 GHz we incorporate the beamed products (blazars) by randomly aligning the sources with respect to our line-of-sight, allowing both different Lorentz factors ( $\gamma$ ) and different core-to-extended flux ratios for the two (FRI,FRII) populations. The best-fit beaming parameters are shown in Table 3.

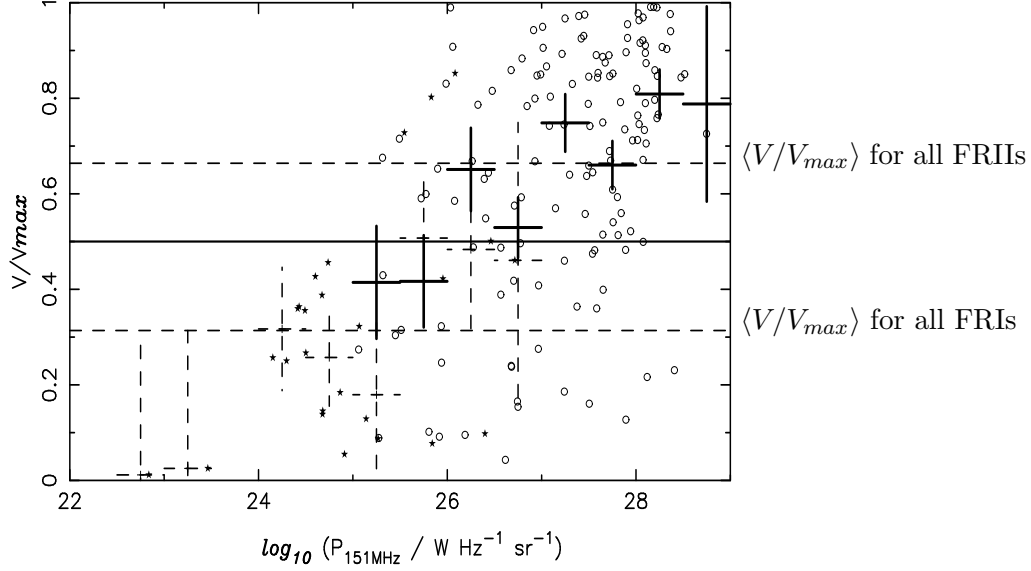


Figure 3.  $V/V_{max}$  for individual 3CRR FRI radio galaxies (★) and FRII radio galaxies (○). Overplotted are  $\langle V/V_{max} \rangle$  values for bins of 0.5 in  $\log_{10}(P_{151 \text{ MHz}})$  for FRIs (dashed +) and FRIIs (solid +).

Table 2. Fitted evolution parameter values at 151 MHz for LDDE:  $\rho(P, z) = \rho_0(P) \exp M(P)\tau(z)$

Population	Exponential LDDE parameter values	Chi-square test	
		$\chi^2_{min}$	$\nu^a$
FRI	$M_{max} = 0.0, z_c = 5.0$ $P_1$ & $P_2$ not used given $M_{max} = 0.0$		
FRII, class A & B	$M_{max} = 10.93, z_c = 5.62$ $P_1 = 25.44, P_2 = 27.34$		
	best-fit	30.73	33

<sup>a</sup> Degrees of freedom

Table 3. Fitted beaming parameter values at 5 GHz

Population	Parameter values	Chi-square test	
		$\chi_{min}^2$	$\nu^a$
FRI	$\gamma = 15.0, R_{med} \propto P_{151 \text{ MHz}}^{-0.55}$		
FR II, class A & B	$\gamma = 8.5, R_{med} = 0.01$ $\theta_c(R_{med}) = 7^\circ.1$		
	best-fit	32.98	25

The contribution from each population to the 5-GHz source count is shown in Figure 4. The contribution from the quasar population peaks at a higher flux density limit than its parent population, and a similar behaviour is seen for the BL Lac objects.

We can analyse the relative importance of each class of radio source as a function of flux density. Blazars are dominated by quasars (high-excitation FR II parents) at  $S_{5 \text{ GHz}} > 0.3 \text{ Jy}$ , but dominated by BL Lac-type objects at lower flux densities. The magnitude of the rapidly changing quasar fraction predicted by our model is well-matched by observations from the 0.25 Jy-sample of flat-spectrum sources of Shaver et al. (1996) - see Figure 15 of Jackson & Wall (1999).

In terms of population mix, it is also instructive to consider the integral population count, shown in Figure 5 in which the model fit has been transposed to 1.4 GHz. This figure reveals that complete samples are predicted to comprise  $\sim 20\%$  BL Lac objects for flux density limits extending down to  $S_{1.4 \text{ GHz}} \sim 0.1 \text{ mJy}$ . Optical spectroscopy of objects selected from the FIRST survey (Becker, White & Helfand 1995) could provide substantial tests of this prediction to  $S_{1.4 \text{ GHz}} \sim 1 \text{ mJy}$ .

#### 4. Redshift distributions of blazars

Transposing our model (evolution plus beaming) to 2.7 GHz we compare our predictions with the limited observational data currently available. Figure 6 shows the mean redshift,  $\langle z \rangle$ , across a wide flux density limit range for all source types as well as three sub-classes. For complete samples the model predicts that the value of  $\langle z \rangle$  peaks at  $\sim 20 \text{ mJy}$  then drops rapidly. In detail, we find that (i) the contribution from steep-spectrum sources dominates and therefore traces the overall  $\langle z \rangle$ , (ii) for the quasar population,  $\langle z \rangle$  rises continuously as  $S_{2.7 \text{ GHz}}$  decreases. However the *number* of quasars is negligible below  $S_{2.7 \text{ GHz}} = 20 \text{ mJy}$  so this has little effect on the overall  $\langle z \rangle$  value and (iii) the peak  $\langle z \rangle$  of the BL Lac sources occurs at a higher flux density than that of the quasars, although the value of  $\langle z \rangle$  is much lower.

Comparing the model  $\langle z \rangle$  values to the 0.25 Jy flat-spectrum quasar sample of Shaver et al. (1996 and in preparation) we find reasonable agreement. The data points for the 0.25 Jy sample shown on Figure 6 are *lower* limits as this

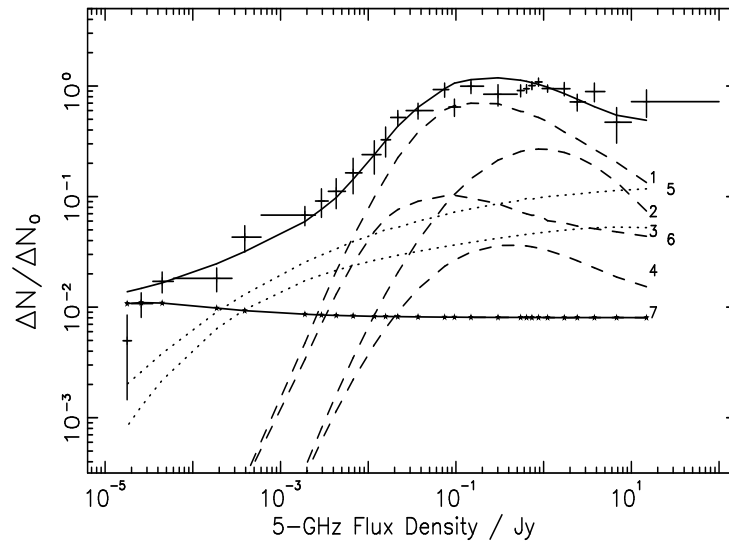


Figure 4. Observed (+) and model (solid line) differential source counts at 5 GHz. The model count comprises 4 contributions from FR II parents (dashed): 1) high-excitation radio galaxies, 2) quasars (from high-excitation parents), 3) low-excitation radio galaxies and 4) BL Lac type objects (from low-excitation parents). There are 2 contributions from FR I parents (dotted): 5) radio galaxies and 6) BL Lac type objects. The contribution from the starburst galaxy population is shown dot-dashed (7).

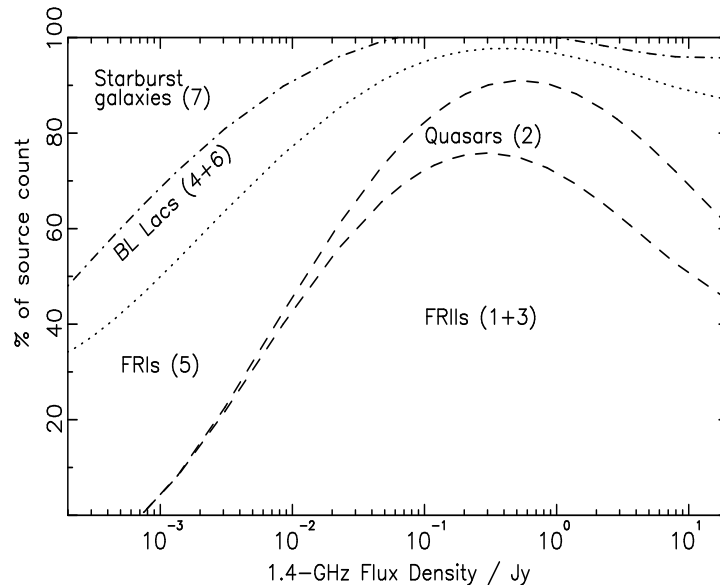


Figure 5. Integral population mix from the model fit at 5 GHz transposed to 1.4 GHz. Numbers in braces refer to the populations described in Figure 4.



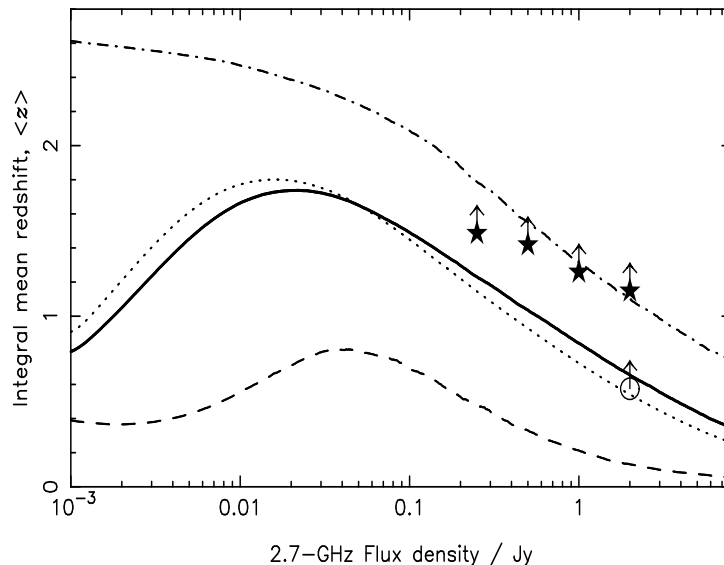


Figure 6. Model  $\langle z \rangle$  of all sources to limiting flux density at 1.4 GHz (solid line). Contributions from the steep spectrum FRII, FRI and starburst galaxies (populations 1, 3, 5, and 7) shown dotted, quasars (from high-excitation FRIIs, population 2) dot-dashed and BL Lacs (from low-excitation FRIIs and FRIs, populations 4 and 6) dashed. Data points are from the flat-spectrum quasar sample ( $\star$ ) (Shaver et al. 1996) and the 2 Jy sample ( $\circ$ ) (Wall & Peacock 1985, Morganti et al. 1997). The solid curve shows the total.

sample selects quasars with ( $\alpha_{2.7\text{ GHz}}^{5\text{ GHz}} > -0.4$ ). Our model, however, defines blazars as having ( $\alpha_{2.7\text{ GHz}}^{5\text{ GHz}} > -0.5$ ). Beamed objects with  $\alpha_{2.7\text{ GHz}}^{5\text{ GHz}} > -0.4$  have parent sources of lower radio luminosity, which in turn are predicted to have a lower  $\langle z \rangle$  distribution than the less-beamed  $-0.5 < \alpha_{2.7\text{ GHz}}^{5\text{ GHz}} < -0.4$ , higher-luminosity objects which are missing from the 0.25 Jy sample.

The  $\langle z \rangle$  value for the complete 2-Jy sample (Wall & Peacock 1985, Morganti et al. 1997) agrees well with the overall  $\langle z \rangle$  model prediction.

Figure 7 splits the BL Lac  $\langle z \rangle$  distribution of Figure 6 into its contributing parent populations. We see that low-excitation-FRII BL Lac sources have a  $\langle z \rangle$  distribution which is very similar to the quasar distribution. However, the FRI BL Lacs have a very different distribution, with  $\langle z \rangle$  gradually increasing with decreasing flux density. Morphological studies of a sizeable sample of BL Lac objects from *e.g.* the FIRST survey would provide direct, powerful tests of this prediction.

## References

- Barthel, P. D. 1989, *ApJ*, 336, 606  
 Benn, C. R., Rowan-Robinson, M., McMahon, R. G., Broadhurst, T. J., & Lawrence, A. 1993, *MNRAS*, 263, 98

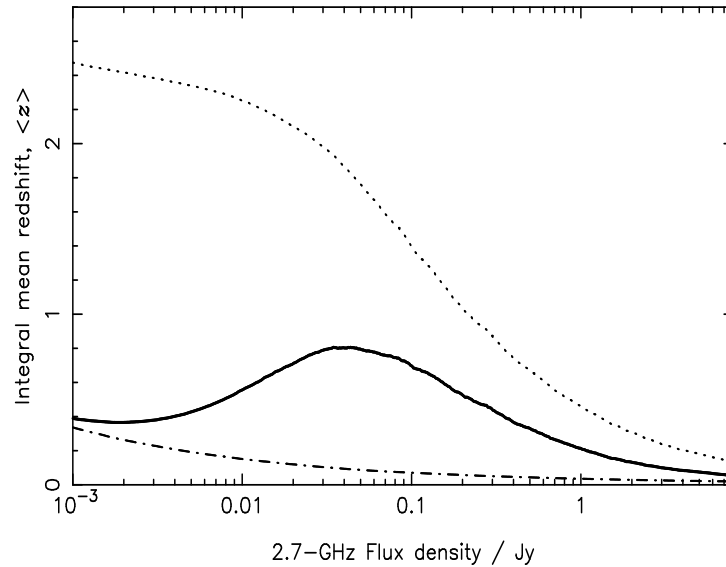


Figure 7. Model mean redshift of BL Lacs from their two parent populations – low-excitation FRIIs (population 4) dotted, FRIIs (population 6) dot-dashed.

- Fanaroff, B. L., & Riley, J. M. 1974, MNRAS, 167, 31P  
Hales, S. E. G., Baldwin, J. E., & Warner, P. J. 1988, MNRAS 234, 919  
Hine, R. G., & Longair, M. S. 1979, MNRAS, 188, 111  
Jackson, C. A., & Wall, J. V. 1999, MNRAS, 304, 160  
Laing, R. A., Riley, J. M., & Longair, M. S. 1983, MNRAS, 204, 151  
Longair, M. S. 1966, MNRAS, 133, 421  
Morganti, R., Oosterloo, T. A., Reynolds, J. E., Tadhunter, C. N., & Migenes, V. 1997, MNRAS, 284, 541  
Orr, M. J. L. & Browne, I. W. A. 1982, MNRAS, 200, 1067  
Owen, F. N. & Ledlow, M. J. 1994, in *The Physics of Active Galaxies*, eds Bicknell, G. V. et al., ASP Conf. Ser., 54, 319  
Ryle, M., & Clarke, R. W. 1961, MNRAS 122, 349  
Scheuer, P. A. G. 1987, in *Superluminal Radio Sources*, ed. J. A. Zensus & T. J. Pearson, CUP, Cambridge, 104  
Scheuer, P. A. G., & Readhead, A. C. S. 1979, *Nature*, 277, 182  
Shaver, P. A., Wall, J. V., Kellermann, K. I., Jackson, C. A., & Hawkins, M. R. S. 1996, *Nature*, 384, 439  
Urry, C. M. & Padovani, P. 1995, *PASP*, 107, 803  
Wall, J. V., & Jackson, C. A. 1997, MNRAS, 290, L17  
Wall, J. V., & Peacock, J. A. 1985, MNRAS, 216, 173  
Windhorst, R. A., Fomalont, E. B., Partridge, R. B., & Lowenthal, J. D. 1993, *ApJ*, 405, 494